In vitro and in vivo synergy of MCP compounds with mitogen-activated protein kinase pathway– and microtubule-targeting inhibitors

Natalia Skobeleva,[1,2] Sanjay Menon,[3] Lutz Weber,[3] Erica A. Golemis,[1] and Vladimir Khazak[3]

[1]Division of Basic Sciences, Fox Chase Cancer Center, Philadelphia, Pennsylvania; [2]Petersburg Nuclear Physics Institute, St. Petersburg, Russia; and [3]NexusPharma, Inc., Langhorne, Pennsylvania

Abstract

An important clinical task is to coherently integrate the use of protein-targeted drugs into preexisting therapeutic regimens, with the goal of improving treatment efficacy. Constitutive activation of Ras-dependent signaling is important in many tumors, and agents that inhibit this pathway might be useful in numerous therapeutic combinations. The MCP compounds were identified as inhibitors of Ras-Raf interactions and previously shown to inhibit multiple Ras-dependent transformation phenotypes when used as monoagents in cell culture analyses. In this study, we investigate the ability of the MCP110 compound to synergistically enhance the activity of other therapeutic agents. In both a defined K-Ras–transformed fibroblast model and in human tumor cell lines with mutationally activated Ras, MCP110 selectively synergizes with other agents targeting the mitogen-activated protein kinase pathway, and with multiple agents (paclitaxel, docetaxel, and vincristine) targeting the microtubule network. The synergistic activity of MCP110 and paclitaxel was further established by experiments showing that in Kaposi's sarcoma oncogenically transformed cell lines, cellular models for tumors treated with taxanes in the clinic and in which Raf-dependent signaling plays an important role, MCP110 synergizes with paclitaxel and limit growth. Finally, in vivo testing indicate that MCP110 is bioavailable, inhibits the growth of LXFA 629 lung and SW620 colon carcinoma cells in xenograft models, and again strongly synergizes with paclitaxel. Together, these findings indicate that MCP compounds have potential to be effective in combination with other anticancer agents. [Mol Cancer Ther 2007;6(3):898–906]

Introduction

Activation of the Ras oncoprotein is a critical element in many different cancers, including pancreatic, breast, and others (reviewed in ref. 1). In some tumors, Ras is directly activated by mutation, whereas in others the constitutive signaling of upstream regulatory factors, such as the epidermal growth factor receptor, promote deregulated activation of wild-type Ras (2). Active Ras promotes tumor growth through its ability to activate multiple downstream effector signaling pathways that promote cell proliferation, survival, migration, and angiogenesis (reviewed in refs. 3, 4). Among these different pathways, Ras interaction with and activation of Raf serine/threonine kinases (Raf-1, A-Raf, and B-Raf), phosphatidylinositol 3-kinases, and Ral guanine nucleotide exchange factors has been shown to be critical for tumor promotion. Although different tumor types rely to differing degrees on activation of the Raf, phosphatidylinositol 3-kinase, and Ral guanine nucleotide exchange factor effector pathways (5), the particular importance of Raf activation has long been appreciated (6). For these reasons, strategies to rationally design chemotherapeutic agents that specifically antagonize the Ras/Raf/extracellular signal-regulated kinase (ERK) kinase (MEK)/ERK signaling cascade have been considered to be promising (6).

The MCP1 compound was isolated based on its ability to block the interaction of Ras and Raf-1 in a yeast two-hybrid assay (7). In initial characterizations of the efficacy of MCP1 and a more potent derivative, MCP110, both were shown to efficiently reverse multiple Ras-dependent transformation changes in mammalian cells (7, 8). This analysis showed that MCP compounds inhibited Ras-induced activation of the Raf and ERK mitogen-activated protein kinase (MAPK) signaling cascade, Ras-induced cell migration, morphologic changes and anchorage-independent growth, and Ras-regulated expression of matrix metalloproteases and cyclin D1 (7). Based on these results, this class of compounds was selected for further evaluation.

Very few clinical agents are successful as monotherapies; instead, dual or triple-therapies are generally significantly more potent. Modern therapeutic combination strategies fall into four categories. In one approach, a single signaling pathway is "vertically" targeted, with drugs inhibiting multiple steps in a signaling cascade: For example, pretreatment of A549 lung carcinoma cells with the phosphatidylinositol 3-kinase inhibitor PX-866, which

strongly potentiates the action of the epidermal growth factor receptor inhibitor Iressa (9). In a second, ''horizontal,'' approach, two or more cooperating signaling pathways are targeted in parallel. Synergistic effect has been documented in glioblastoma cells treated with Raf-1 or MEK kinase inhibitors (GW5074 and U0126) together with ILKAS, an antisense oligonucleotide that inhibits the phosphatidylinositol 3-kinase–regulated ILK and AKT kinases (10). A third approach is the use of multiple agents for the same target. For example, Cetuximab and Iressa (an antibody and a small-molecule inhibitor of epidermal growth factor receptor) showed a marked synergistic effect in a phase II clinical trial in colon carcinoma (11). A final approach is the combination of a pathway-targeted drug with a conventional cytotoxic agent. For example, the humanized anti-Her2 antibody herceptin (trastuzumab) productively synergizes with cisplatin and taxanes to treat breast cancer (12, 13).

In this study, we have assessed the efficacy of MCP110 in enhancing the activity of established clinical agents and probed the mode of action of MCP110. Our data indicate that MCP110 synergizes both with other small molecules targeting the MAPK pathway and with multiple mitotic spindle-targeting agents. This synergy occurs *in vitro* and *in vivo*, and is observed in multiple cancer models relevant to activation of Ras signaling. These studies predict that MCP compounds are potentially useful additions to the clinical armamentarium.

Materials and Methods

Cell Lines and Plasmids

Cells used included SW620 cells (American Type Culture Collection, Manassas, VA), endothelial cell (EC)-vGPCR (14), and NIH3T3 cells stably transfected with the pBabe-puro retrovirus vector or expressing constitutively activated H-, K-, or N-Ras (15); Raf22W (16); MEK1ΔN3/S222D (15); or KSHV-GPCR (17).

Compounds

MCP1 and MCP110 were synthesized as described previously (8); structures and structure-activity relationships have also been described for these compounds (8). Sorafenib (ref. 18; Calbiochem), U0126 (Promega, Madison, WI), paclitaxel (Biomol, Plymouth Meeting, PA), docetaxel (Fox Chase Cancer Center pharmacy; Sanofi-Aventis, Dublin, Ireland), vincristine (Sigma, St. Louis, MO), AACOCF3 (Biomol), gemcitabine (Shanghai Sunshine International Tdg., Co., Ltd., Shanghai, China), and staurosporine (Sigma) were commercially prepared.

Proliferation, Anchorage Independence, Cell Cycle, and Apoptosis Assays

Proliferation was measured 48 h after addition of compounds to cells using WST-1 reagent (Roche Applied Sciences, Indianapolis, IN) according to standard protocols. Anchorage-independent growth assays were done essentially as described (19). Twelve to 21 days after cell seeding, cells were stained with thiazolyl blue tetrazolium bromide, and colonies >600 μm in diameter were scored using a Nikon SMZ1500 microscope coupled with Cool Snap charge coupled device camera (Roper Scientific, Inc., Tucson, AZ) with Image Pro-Plus software (Media Cybernetics, Silver Spring, MD). Survival curves were based on at least six concentration points, with values determined in at least three separate experiments, with each assay done in sextuplicate. All statistical analysis was done using the Excelfit software program (ID Business Solution, Inc., Bridgewater, NJ), with the exception that drug combinations were investigated for synergy, additive effect, or antagonism using median dose effect analysis as in ref. (20) by using CalcuSyn software (Biosoft, Ferguson, MO) to establish the combination index (CI). Cell cycle compartmentalization and apoptotic index were determined using fluorescence-activated cell sorting analysis using FACSII instrument (BD Biosciences, Franklin Lakes, NJ), using standard approaches. Apoptotic cells were detected by staining with antibody to Annexin V (BD Bioscience PharMingen, San Jose CA).

Compound Formulation for *In vivo* Application in Severe Combined Immunodeficient Mice Xenografts

Both MCP110 and paclitaxel were administered in a liposomal formulation containing 10% (w/v) phospholipon 90G (American Lecithin Company, Oxford, CT) and 33% (v/v) Myritol 318 (Cognis Corp., Cincinnati, OH). Details of preparation of the formulation are available on request.

Pharmacokinetics and Maximum Tolerated Dose Assessment in Nude Mice

To determine the *in vivo* bioavailability of MCP1 and MCP110 administered through different routes, groups of 12 NMRI nu/nu mice received a single dose of compounds formulated in 100% ethanol and 10% hydroxypropyl-β-cyclodextrin. For the p.o. route, the dose level was chosen at 30 mg/kg and clinical signs were documented immediately before dosing and at 0.5, 1, 2, and 5 h after dosing. Compound plasma concentrations were determined at 0.5, 1, 2, and 5 h after dosing. For i.p. and i.v. routes, the compounds were tested at a dose level of 3 mg/kg, and clinical signs and compound plasma concentrations were documented before dosing, and 10 min, 20 min, 1 h, and 3 h after dosing. For determining the blood plasma concentrations, an internal standard was added to all plasma samples: compounds were detected using high-performance chromatography-mass spectrometry/mass spectrometry analysis with a PE/SCIEX API3000 instrument.

For maximum tolerated dose assessment, groups of NMRI nu/nu mice received a single i.p. injection of MCP110 at dose levels specified in the results, or vehicle [20% DMSO, 5% Cremophor EL, 75% hydroxypropyl-β-cyclodextrin (Yiming Fine Chemicals, Ltd., Jiangsu, China)], and a solution composed of 10% Myritol 318 (v/v) and 3% Phospholipon 90G (w/v) in water. For 7-day repetitive dose studies, MCP110 was delivered at 0, 300, 600, and 1,200 mg/kg/d, with dosing followed by a 4- or 16-day observation period. Doses were administered at a volume of 10 mL/kg/d.

Tumor Xenograft Analysis in Athymic (nu/nu) Nude and Severe Combined Immunodeficient Mice

SW620 colon carcinoma and LXFA 629 NSCLC cells were used to induce xenografts in 4- to 6-week-old severe

combined immunodeficient and athymic nude males. Studies with LXFA 629 cells were done by Oncotest (Freiburg, Germany). Exponentially growing cells were harvested, washed with PBS, and resuspended in DMEM. Cells (2.5×10^6 to 5×10^6) were transplanted s.c. into the right flank of each mouse (5–10 mice per group). Animals were monitored for 3 weeks for tumor formation before treatment. During treatment, MCP compounds were injected daily; paclitaxel was included in 8 of 17 injections (see Results). For analysis, tumor volume was determined by measuring ($L \times W \times W$) / 2, where L and W represent the longest length and width of the tumor, respectively. Tumor growth inhibition was measured as the median tumor weight of the treated group (T) divided by the median tumor weight of the control group (C) at the time when the median tumor weight in the control group has reached ~700 mg and expressed as the T/C value. A standard Mann-Whitney-Wilcoxon U test was used to establish significant differences in the ranking of individual tumors.

Results

Synergy of MCP110 with Ras ⟩ Raf ⟩ MEK1 ⟩ MAPK Pathway Inhibitors in Ras-Transformed Cells

We first evaluated the ability of MCP110 to synergize with agents that vertically target the Ras > Raf > MEK > ERK pathway versus their ability to synergize with compounds that targeted unrelated signaling pathways. Sorafenib (BAY 43-9006) inhibits Raf kinase (and additional kinases; ref. 21), and U0126 specifically inhibits MEK1 kinase (22). In the NIH3T3-K-Ras(G12V) model, the IC_{50} values of these compounds used as monoagents are 17 μmol/L (MCP110), 10.3 μmol/L (sorafenib), and 47.6 μmol/L (U0126) in a proliferation assay and 8.1 μmol/L (MCP110), 9.3 μmol/L (sorafenib), and 12.4 μmol/L (U0126) in a soft agar colony-formation assay. We observed a dose-dependent growth inhibition effect when NIH3T3-K-Ras(G12V) cells were treated with the combination of 10 μmol/L MCP110 with U0126 or sorafenib in both proliferation (Fig. 1A) and colony-formation (Fig. 1B) assays, with the colony-formation assay showing a more pronounced effect of combination.

For comparison, we used the more sensitive colony-formation assay to analyze the combination of MCP110 with a set of small-molecule agents with molecular targets not directly related to Ras transformation. These included staurosporine (a protein kinase C inhibitor with additional off-target activities), gemcitabine (a DNA synthesis inhibitor), and AACOCF3 (a cPLA2 inhibitor; cPLA2 is a component of a side feedback regulation loop for the MAPK pathway; ref. 23). IC$_{50}$ values for compounds used as monagents were 37.0 μmol/L (AACOCF3), 1.4 nmol/L (staurosporine), and 58.3 nmol/L (gemcitabine). Staurosporine and gemcitabine exhibited neither synergistic nor additive effect with MCP110 (Fig. 1C). AACOCF3 had a weak additive activity, although much less than was seen with sorafenib or U0126.
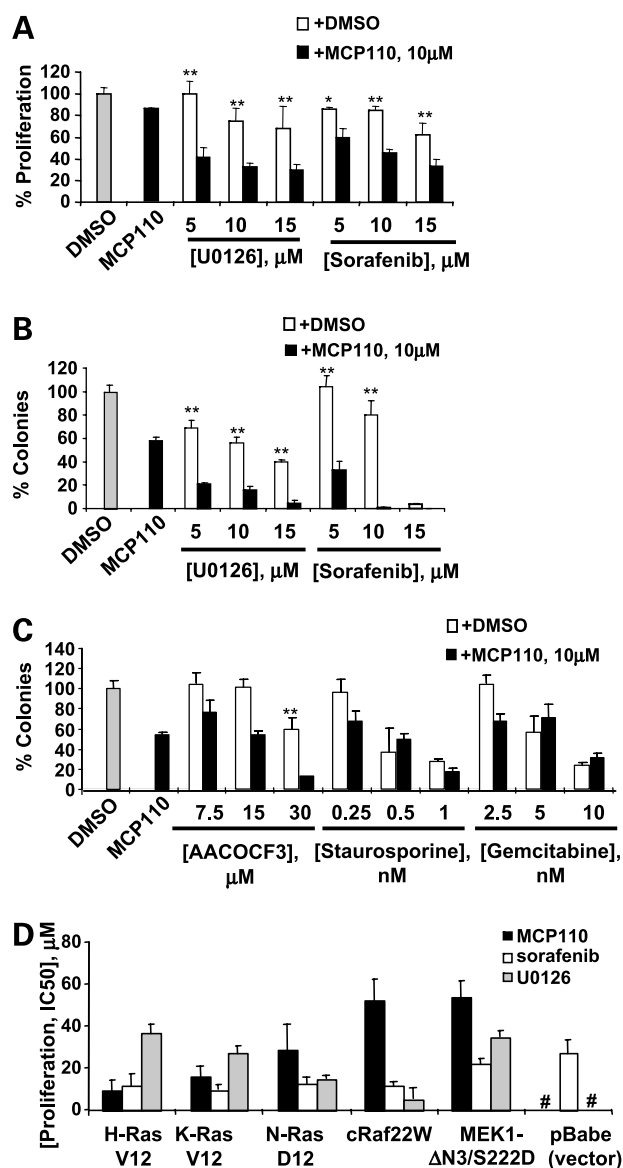

Figure 1. Specific synergy between MCP110 and other agents targeting the MAPK pathways in NIH3T3-K-Ras(G12V) cells. **A,** the proliferation of cells in DMSO-treated plates was taken as 100%, and the number of cells in compound-treated plates was expressed as the percentage of this value for this and the following experiments. Then, proliferation was assessed for NIH3T3-K-Ras(G12V) cells treated with DMSO vehicle (*gray column*), MCP110 at 10 μmol/L delivered as monoagent, or with U0126 or sorafenib at 5, 10, or 15 μmol/L in combination with DMSO (*white columns*) or MCP110 at 10 μmol/L (*black columns*). *, $P < 0.05$; **, $P < 0.001$. **B,** assay design was as in **A,** except that colony-forming potential was assayed. *, $P < 0.05$; **, $P < 0.001$. **C,** the same experimental design was used as in **A,** except that the concentrations of AACOCF3, staurosporine, and gemcitabine were as indicated. **D,** IC$_{50}$ values for inhibition of proliferation were determined for each cell line in reference to a DMSO control. #, no significant growth inhibition at >60 μmol/L.

If MCP110 action is specifically related to its ability to inhibit the Ras-Raf interaction, MCP110 should be potent in cell lines transformed by Ras but not transformed by oncogenes acting downstream of the Ras-Raf interaction.

We analyzed MCP110 activity in NIH3T3 cells transformed by constitutively active H-Ras(G12V), K-Ras(G12V), and N-Ras(G12D). For comparison, we also examined activity of MCP compounds in cells transformed by Raf22W (16), a constitutively activated Raf-1 derivative truncated to lack Ras-interacting sequences, or by catalytically activated MEK1ΔN3/S222D (15); or in NIH3T3 cells containing expression vector (pBabe-puro). This analysis (Fig. 1D) showed significantly greater potency of MCP110 in Ras-transformed versus Raf- or MEK1-transformed cell lines, and no activity of MCP110 in the vector-control cell line. This contrasted with sorafenib and U0126, which were active in all transformed cell lines.

Synergy of MCP110 with Microtubule-Targeting Agents

Paclitaxel is widely used in the treatment of lung, ovarian, and breast carcinomas (24). Although a primary mode of action of paclitaxel is as a cytotoxic agent that disrupts microtubule dynamics, paclitaxel also modulates Raf-1 activation, and paclitaxel efficacy has been defined as partially dependent on Raf-1 status (25–31). The paclitaxel IC_{50} for inhibition of proliferation in NIH3T3-K-Ras(G12V) cells is 930 nmol/L for proliferation and 46 nmol/L for soft agar colony formation. Combination of paclitaxel with low doses of MCP110 produced a very striking reduction of cell proliferation and colony formation (Fig. 2A and B). In complementary analysis, we generated colony-formation IC_{50} curves for paclitaxel in the presence of 1 or 10 μmol/L MCP110, sorafenib, or U0126 (Fig. 2C). Treatment with 1 μmol/L MCP110 reduced the paclitaxel IC_{50} from 46 to 10.7 nmol/L; treatment with 10 μmol/L MCP110 reduced the paclitaxel IC_{50} to 1 – 1.5 nmol/L (Fig. 2C). A significantly greater synergy was observed between paclitaxel and MCP110 than with paclitaxel and sorafenib or U0126. MCP110 also strongly potentiated the action of two additional microtubule-targeting agents, docetaxel and vincristine (Fig. 2D), suggesting a broad utility in combination with this inhibitor class.

We have found that significantly more Annexin V–positive, apoptotic cells were found after combined MCP110 and paclitaxel treatment than in cells treated with either agent alone (Fig. 3A). Induction of cell death by microtubule-targeting agents is most potent when treated cells are in mitosis (32, 33). Using fluorescence-activated cell sorting analysis, we analyzed the cell cycle compartmentalization of NIH3T3-K-Ras(G12V) cells treated with MCP110, paclitaxel, or both (Fig. 3B). For reference, we compared cell cycle compartmentalization of NIH3T3-K-Ras(G12V) cells treated with U0126 and paclitaxel (Fig. 3B), or the NIH3T3-Raf22W cell lines in which MCP110 compounds were inactive with both (Fig. 3C). Intriguingly, MCP110 administered in combination with paclitaxel significantly increased the percentage of cells in the G_2-M compartment although MCP110 used as monoagent did not affect cell cycle compartmentalization at the concentrations tested, and this effect was specific to the K-Ras(G12V)–transformed cell line. The combination of U0126 and paclitaxel did not have this effect in either cell line.
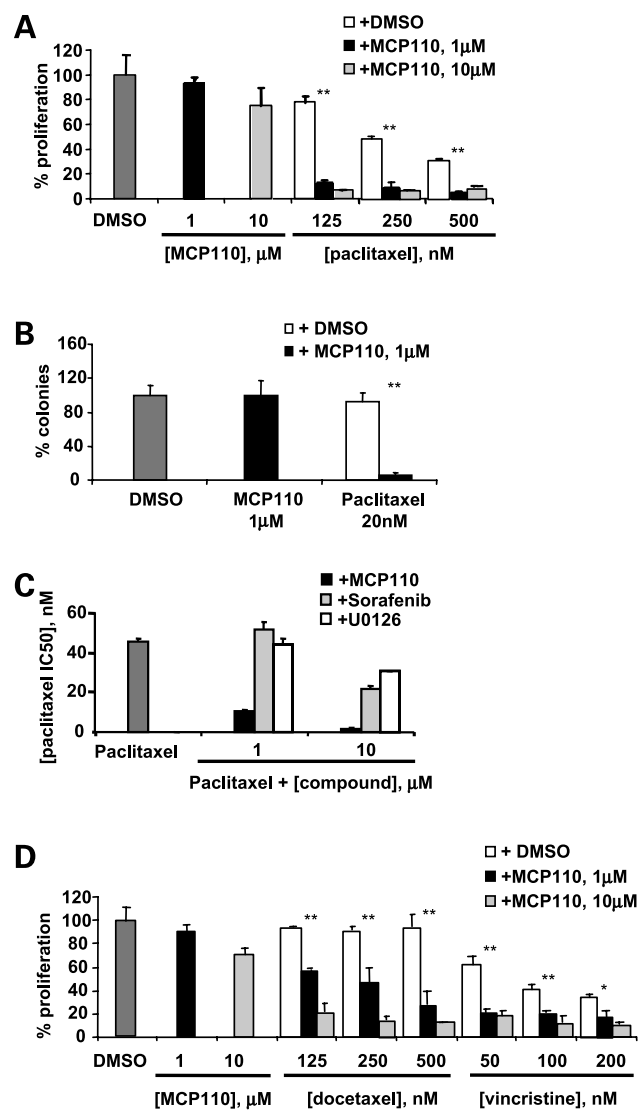

Figure 2. MCP1 and MCP110 compounds synergize with paclitaxel and other microtubule-targeting agents in inhibition of anchorage-dependent and anchorage-independent growth in NIH3T3-K-Ras(G12V) cells. **A,** proliferation assay was done in Fig. 1A, except the use of MCP110 and paclitaxel at the values indicated. **, $P < 0.001$. **B,** a colony-formation assay was done as in Fig. 1B, except the use of MCP110 and paclitaxel. **, $P < 0.001$. **C,** paclitaxel was administered to cells in combination with DMSO (*dark gray column*) or MCP110 (*black columns*), sorafenib (*light gray columns*), and U0126 (*white columns*) at 1 or 10 μmol/L, as indicated. **D,** proliferation assay was done as in **A**, except using docetaxel and vincristine at the indicated concentrations. IC_{50} values for docetaxel and vincristine used as monoagents were 303 and 270 nmol/L, respectively. *, $P < 0.05$; **, $P < 0.001$.

Sensitivity of Human Cancer Cell Lines to MCP Compounds, Paclitaxel, and MCP-Paclitaxel Combination

Requirements for Ras-dependent signaling in transformation differ between humans and mice, and between fibroblasts and epithelial cells (5, 34, 35). To determine whether MCP compounds are effective as single and combination agents in human cancers as well as in defined transformation models, we analyzed a number of human
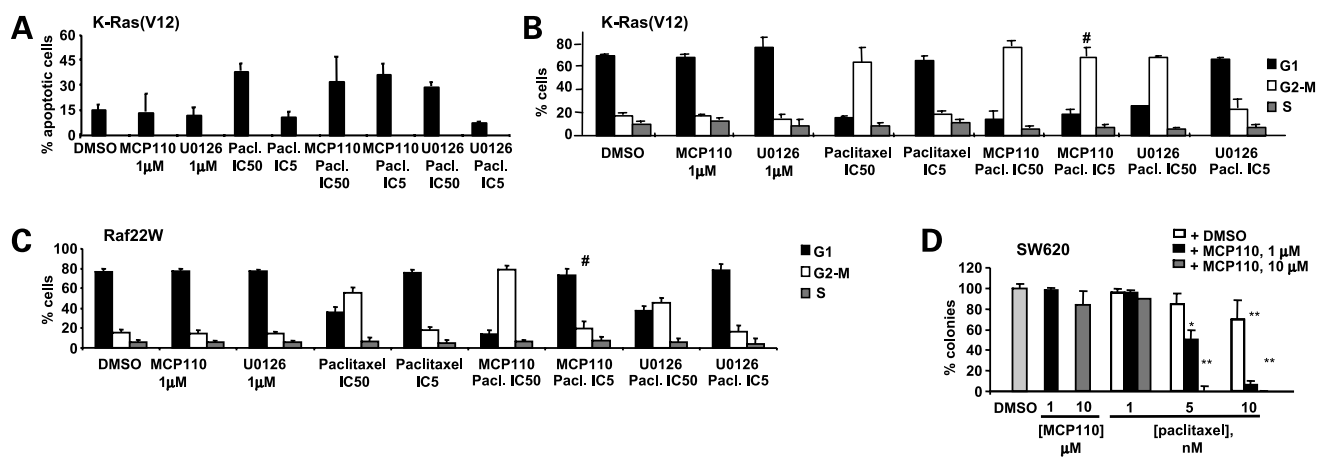
Figure 3. Selective action of MCP110 and paclitaxel in Ras versus Raf-transformed cells. **A,** NIH3T3-K-Ras(G12V) cells were stained with antibody to Annexin V and analyzed by fluorescence-activated cell sorting analysis. For combination experiments, MCP110 and U0126 at indicated concentrations were mixed with paclitaxel at predetermined IC_{50} and IC_5 values for the cell line. **B,** cell cycle compartmentalization of NIH3T3-K-Ras(G12V) cells treated with compounds at the concentrations noted. #, G2 accumulation of MCP110/paclitaxel–treated cells. **C,** experiment as in **B,** except the use of NIH3T3-Raf22W cells. #, no G2 accumulation of MCP110/paclitaxel–treated cells. **D,** colony-forming potential of SW620 cells was determined in cells treated with DMSO (*light gray column*), MCP110 at 1 or 10 μmol/L delivered as a monoagent, or with paclitaxel at 1, 5, or 10 nmol/L in combination with MCP110 at concentrations indicated. Values show percentage reduction of colonies in compound-treated cells in reference to DMSO-treated cells. *, $P < 0.05$; **, $P < 0.001$.

cancer cell lines with known activating mutations in Ras, including SW620, HCT116, MDA-MB231, NCI-460, and A549. For each of these cell lines, IC_{50} values for MCP110 ranged between 10 and 15 μmol/L. We used the SW620 colorectal adenocarcinoma cell line, which contained an activating K-Ras(G12V) mutation, for further detailed studies.

Preparatory to *in vivo* analysis, we wished to determine in detail the level of synergy between MCP110, paclitaxel, sorafenib, and U0126 compounds. SW620 cells were treated simultaneously with MCP110 and other drugs at a series of fixed ratios for 48 h in both proliferation (WST-1) or in colony formation in soft agar assays (Table 1). We also measured whether 1 and 10 μmol/L MCP110 sensitized SW620 cells to 1, 5, and 10 nmol/L paclitaxel in soft agar colony formation (Fig. 3D), using the general approach used in Figs. 1 and 2. All approaches clearly showed a strong synergistic effect of MCP110 and paclitaxel on

growth of these cells in both assays in different concentration ratios, and synergistic or strong additive effects between MCP110 and sorafenib and U0126. Although the highest degree of synergy was observed between MCP110 and paclitaxel assessed in soft agar, a significant effect was also seen in the proliferation assay. Similar results were obtained in additional cell lines with activated Ras (e.g., A549 and NCI-460 cells; results not shown), supporting the idea that these compounds would combine well in primary human tumors.

Synergy of MCP Compounds with Sorafenib and Paclitaxel in Cell Models for KSHV Transformation

Oncogenic viruses act in part by activating protransformation cellular signaling pathways, with a number of such viruses inducing or dependent on Ras pathway activation. KSHV transformation requires Ras-Raf–dependent signaling (36, 37), and paclitaxel is one of the few treatments currently approved for advanced stages of KSHV infection

Table 1. Synergy of MCP110 with U0126, sorafenib, and paclitaxel in SW620 human colon carcinoma cells

Combination	Ratio	Assay	CI(ED$_{50}$)	CI(ED$_{75}$)	CI(ED$_{90}$)	Avg CI
MCP110-U0126	2.1/1	WST-1	0.74	0.47	0.35	0.52
MCP110-sorafenib	5.5/1	WST-1	0.85	0.78	0.72	0.78
MCP110-paclitaxel	2,200/1	WST-1	0.64	0.41	0.31	0.45
MCP110-paclitaxel	1,000/1	WST-1	0.69	0.48	0.35	0.51
MCP110-paclitaxel	1,000/1	SA	0.39	0.30	0.24	0.31
MCP110-paclitaxel	300/1	SA	0.28	0.22	0.18	0.23

NOTE: Anchorage-dependent (WST-1) and anchorage-independent growth assays were done after treatment with compounds at the indicated constant ratios. The CI value was calculated for ED_{50}, ED_{75}, and ED_{90} (see Materials and Methods); the average CI value for each combination is also shown. A CI of <0.3 indicates a strong synergistic effect, 0.3 < CI < 0.7 a synergistic effect, 0.7 < CI < 0.9 moderate synergy, 0.9 < CI < 1 additive effect, and CI > 1 antagonistic effect. Concentrations of compounds analyzed were selected based on the discussions in refs. (20, 45, 46).
Abbreviation: SA, soft agar.

(38). We assessed whether MCP110 can block the cell transformation induced by the KSHV G-protein coupled receptor (vGPCR; ORF74), as KSHV-vGPCR is an important contributor to KSHV transforming potential (14, 39) and the activity of this protein requires Ras-dependent signaling (39, 40). We established IC_{50} for MCP110 and paclitaxel as single agents for proliferation (19.7 µmol/L and 750 nmol/L, respectively) and soft agar colony formation (13.8 µmol/L and 65.5 nmol/L, respectively) in NIH3T3-vGPCR cells (17). Figure 4A and B shows that MCP110 markedly reduced the IC_{50} of paclitaxel in these cells. KSHV-induced cancers are marked by the action of the vGPCR in promotion of vascular endothelial growth factor–driven angiogenesis. We also analyzed MCP110 action in the EC-vGPCR KSHV model (14). IC_{50} for MCP110 and paclitaxel in proliferation assays were 20.2 µmol/L and 250 nmol/L, respectively, in EC-vGPCR cells. Figure 4C shows similar potent action of MCP110 in reducing paclitaxel IC_{50} in this cell line. In these activities, MCP110 was more potent than sorafenib, and significantly more potent than U0126 used at similar concentrations (Fig. 4A–C).

MCP Compound Bioavailability and Maximum Tolerated Dose Assessment

To support the clinical development of an MCP-based analogue, we first established the bioavailability and maximum tolerated dose for the prototype lead compound MCP110, using the related compound MCP1 as a reference. MCP110 was well tolerated after p.o., i.v., and i.p. administration in nude mice, and i.v. and i.p. bioavailability values ranged from moderate to almost complete (64–100%; Fig. 5A and B). MCP110 persisted in the plasma at 16.6% of initially detected levels 3 h after administration by i.p., and 0.72% of initially detected levels when it was administrated by i.v. By contrast, the plasma concentration of MCP1 dropped sharply by 1 h after injection, and MCP1 was undetectable by 3 h postinjection.

Acute dose toxicity and repeated dose toxicity were established. NMRI nu/nu mice received a single i.p. injection of MCP110 in vehicle at dose levels of 0, 600, or 1,000 mg/kg, at a consistent dose volume of 10 mL/kg. Observation of mice for 14 days subsequent to injection indicated that mice tolerated a single i.p. dose of up to 1,000 mg/kg MCP110. Based on this finding, a 7-day repeat dose study using MCP110 at 0, 300, 600, and 1,200 mg/kg/d in constant dose volumes was done, followed by 16 days of observation. Treatment-related changes in body weights were observed during the treatment period in mice that received 1,200 and 600 mg/kg/d, but not 300 mg/kg/d. These changes were dose dependent and resulted in an absence of body weight gain at 600 mg/kg/d, and weight loss at 1,200 mg/kg/d. Three of four males and one of four females treated with MCP110 at 1,200 mg/kg/d survived until day 9 for scheduled sacrifice. Microscopically, there were no changes observed in the surviving female treated at 1,200 mg/kg/d. The males treated at 1,200 mg/kg/d presented minimal to slight changes in the kidney and testes. Shortly after cessation of treatment, all surviving animals for each dose used showed a normal body weight
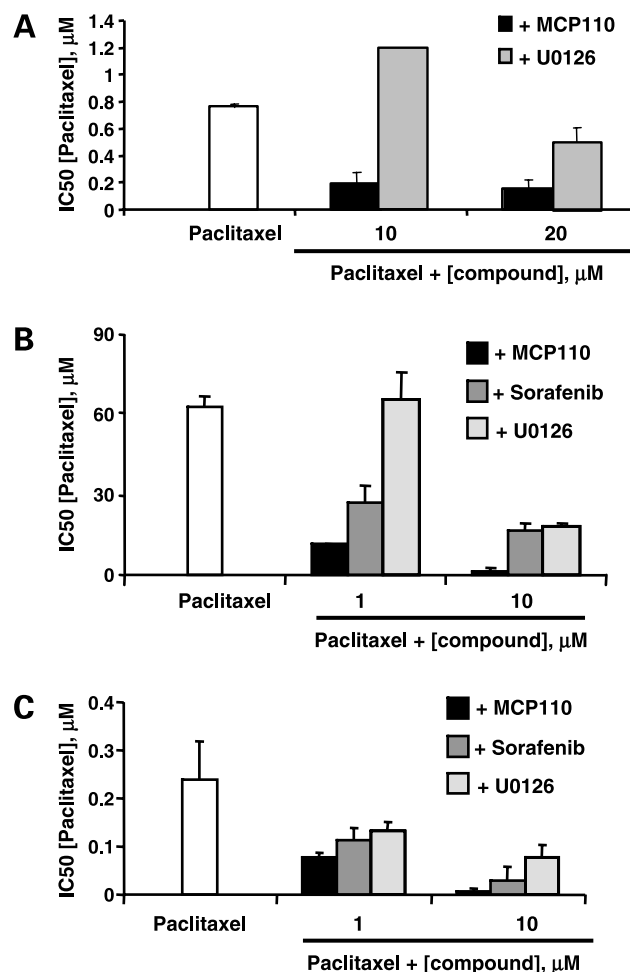

Figure 4. MCP110 effectively synergizes with paclitaxel to inhibit anchorage-dependent and anchorage-independent growth of two distinct KSHV-GPCR–transformed cell lines. **A,** proliferation assays were done in NIH3T3-KSHV cells treated with paclitaxel alone (*white column*), or in combination with MCP110 (*black columns*) or U0126 (*light gray columns*) at the indicated concentrations. IC_{50} values determined for U0126 as monoagent was 20 µmol/L. **B,** colony-formation assays were done in NIH3T3-KSHV cells treated with paclitaxel alone (*white column*), or in combination with MCP110 (*black columns*), sorafenib (*dark gray columns*), or U0126 (*light gray columns*). IC_{50} values determined for sorafenib and U0126 used as monoagents were 15 and 20 µmol/L, respectively. **C,** paclitaxel IC_{50} values were determined in proliferation assays done in EC-vGPCR cells incubated with paclitaxel alone (*white column*) or in combination with MCP110 (*black columns*), sorafenib (*dark gray columns*), or U0126 (*gray columns*) at 1 and 10 µmol/L. IC_{50} values determined for sorafenib and U0126 used as monoagents were 15 and 54 µmol/L, respectively. Note that EC-vGPCR cells do not form colonies in soft agar, so anchorage-independent growth could not be investigated.

gain. Thus, the maximum tolerated repeat dose of MCP110 was established between 600 and 1,200 mg/kg/d, and dose levels of 600 mg/kg/d or lower were used for future repeat dose studies with MCP110.

MCP110 Inhibits the Growth of LXFA 629 Lung Adenocarcinoma Xenografts in Nude Mice

MCP110 was administered i.p. to male NMRI nu/nu mice bearing an established xenograft of the lung adenocarcinoma

cell line LXFA 629. A control group received vehicle only on days 0 to 20 (group 1). Dose levels (in mg/kg/d) were 600 mg/kg on days 0 to 5 and 14 to 18 (group 2); and 300 mg/kg on days 0 to 18 (group 3). Tumor volumes were measured at 3-day intervals for up to 21 days. A reduction in the growth rate of LXFA 629 tumor xenografts relative to the
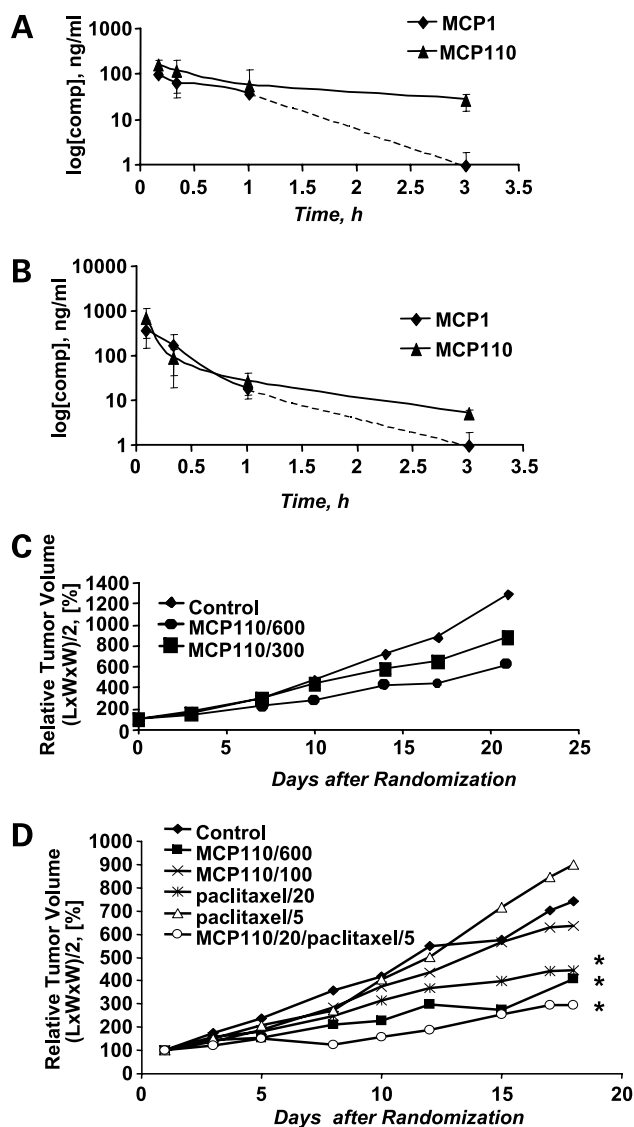

growth rate in the vehicle control group was observed by day 17, with T/C values (ratio of median relative tumor volumes in test and control groups) of 49.3% and 73.8% for groups 2 and 3, respectively (Fig. 5C). A Mann-Whitney-Wilcoxon U test showed significant differences in the ranking of individual tumors according to size between groups 2 and 3, and between both MCP110 treatment groups and the vehicle control group. Other arguments in favor of significant compound-mediated tumor inhibition are (*a*) a continuous increase of T/C values during periods of treatment and (*b*) dose-dependent antitumor activity apparent from comparison of T/C values beginning by the 1st week of treatment.

MCP110 Potently Sensitizes SW620 Human Colorectal Carcinoma Cells to Paclitaxel *In vivo*

To assess MCP110/paclitaxel synergy *in vivo*, we first analyzed the effect of *in vivo* treatment of SW620 xenografts with MCP110 or paclitaxel alone. SW620 cells were implanted into the right flank of male severe combined immunodeficient mice. Palpable tumors of 5 to 14 mm diameter appeared after 2 to 3 weeks, after which animals were randomized to treatment groups, and tumor volume was measured at 3-day intervals for up to 18 days to assess treatment efficacy (Fig. 5D). Control group mice were injected i.p. with vehicle daily for 17 days starting from the time of animal randomization (control). Group 2 (*MCP110/600*) received 600 mg/kg/d MCP110 daily during 17 days of the study. Similarly, animals were treated with 300 mg/kg/d (group 3, data not shown) and 100 mg/kg/d MCP110 (group 4, *MCP110/100*). In groups 5 and 6, animals were treated with 20 or 5 mg/kg/d paclitaxel on days 1, 3, 5, 8, 10, 12, 15, and 17. The data indicated that 100 mg/kg/d MCP110 and 5 mg/kg/d paclitaxel did not significantly limit tumor growth ($P > 0.5$), whereas both 300 and 600 mg/kg/d MCP110 strongly limited tumor growth ($P < 0.05$). Paclitaxel at 20 mg/kg moderately reduced tumor growth, although not to the same extent as 600 mg/kg MCP100; animals dosed with this level of paclitaxel showed signs of distress, including descending colon (by autopsy). T/C values of 55%, 68%, 86%, 60%, and 121% were observed for groups 2, 3, 4, 5, and 6, respectively.

Based on these results, we selected concentrations of 20 mg/kg MCP110 and 5 mg/kg paclitaxel to evaluate potential combination synergy. In group 7 (Fig. 5D, *MCP110/20/paclitaxel/5*), MCP110 was administered daily for 17 days, with paclitaxel administered on days 1, 3, 5, 8, 10, 12, 15, and 17. Within 9 days, a striking reduction in the growth rate of SW620 tumor xenografts relative to the vehicle control group was observed, with T/C values of 40% at 18 days after initiation of dosing (Fig. 5D). This synergistic effect clearly exceeded that seen with either drug used as monoagent at 4- to 5-fold higher concentrations (*MCP110/20/paclitaxel/20* versus *paclitaxel/20*, $P = 0.039$).

Figure 5. MCP110 is bioavailable *in vivo*, is nontoxic, and synergizes with paclitaxel to inhibit tumor growth. The concentrations of MCP1 and MCP110 compounds in mouse plasma were determined after compound administration via i.p. (**A**) or i.v. (**B**) routes. **C,** LXFA 629 nude mice bearing xenografts of LXFA 629 cells were randomized and treated via an i.p. route with vehicle control, or MCP110 at doses of 300 or 600 mg/kg (see Materials and Methods). Relative tumor volume was calculated based on the formula ($L \times W \times W$) / 2 and taken as 100% at the day of randomization. Mean values of groups of 5 to 12 animals were plotted for each dose. **D,** severe combined immunodeficient mice with xenografts of SW620 cells were randomized and treated via an i.p. route with vehicle control, 100 or 600 mg/kg MCP110, 20 or 5 mg/kg paclitaxel, or with a combination of MCP110 at 20 mg/kg and paclitaxel at 5 mg/kg. Relative tumor volume was calculated as in **C**. Average values of groups of 5 to 12 animals were plotted for each dose. *, $P < 0.05$.

Discussion

These results indicate that MCP110 show useful synergies with other agents vertically targeting the Ras-dependent

MAPK signaling pathway, and with three microtubule-targeting agents. These synergies were identified in defined mouse model cell lines for Ras and KSHV-GPCR transformation, and cell lines derived from human cancers containing activating Ras mutations (Figs. 1–3). In NIH3T3-K-Ras(G12V) cells treated with MCP110, paclitaxel more effectively caused cells to enter G_2-M and to undergo apoptosis (Fig. 3). Although different cell line models yield differing results (25, 26), a number of studies have indicated that inhibition of the Raf/MAPK signaling pathway specifically increases the sensitivity of cells to Taxol (41, 42), suggesting that one mechanism for MCP110 is through its prevention of Ras-Raf interaction and hence inhibition of Ras/Raf/MEK/MAPK signaling. Data supporting this interpretation include (*a*) our previous biochemical analyses showing MCP110 inhibition of this pathway (7, 8); (*b*) the fact that MCP110 does not synergize with pathway-irrelevant compounds such as staurosporine or gemcitabine (Fig. 2); (*c*) the fact that MCP110 is selectively active in cells transformed with Ras, but not in cells transformed with Raf22W or MEK, or in untransformed cells (Fig. 1D); and (*d*) the fact that G_2-M accumulation is not seen in MCP110/paclitaxel–treated Raf22W-transformed cells (Fig. 3).

Our observation that MCP110 synergizes with paclitaxel in NIH3T3-vGPCR cells whereas U0126 does not (Fig. 3) suggests that the productive activity of MCP110 involves more than inhibition of the MEK/ERK signaling. Recent studies have suggested a specific importance of activation of the Raf kinase in antiapoptotic signaling that extends beyond its ability to activate MEK/ERK (43). MCP110, acting higher in the Ras signaling pathway than MEK-targeted agents, may be particularly able to block such protumorigenic functions. Because the MCP compound class was identified based on its activity as a protein interaction-inhibitor (7, 8), it is more likely to have a specific target than an active site–targeted kinase inhibitor. Nevertheless, our data do not rigorously exclude the possibility that MCP110 has additional "off-target" activities that contribute to its efficacy (as do many drugs, including sorafenib that is analyzed here; ref. 21); this remains to be determined.

Importantly, MCP110 was bioavailable after i.p. or i.v. administration and was well-tolerated *in vivo*. MCP110 had a measurable antitumor activity in LXFA 629 xenografted mice, when administered at dose levels near the maximum tolerated dose, and treatment with MCP110 as a single agent also caused clear dose-dependent inhibition of tumor growth in SW620 (K-RasV12) severe combined immunodeficient mice xenografts. The most striking result of the study was the drastic reduction in SW620 tumor volume achieved using a combination of MCP110 and paclitaxel, at concentration levels at which neither of the compounds produced significant tumor growth inhibition, indicating a clear synergistic response *in vivo*. The low dose of MCP110 required for synergy with paclitaxel *in vivo* (20 mg/kg) compares favorably with doses of sorafenib used in previous studies examining combination potential of this

agent (40 mg/kg; ref. 44); notably, sorafenib has been successfully developed as a clinical agent. In summary, the obtained data strongly imply that MCP compounds and their analogues are excellent targets for further development toward the clinic.

References

1. Bos JL. ras oncogenes in human cancer: a review. Cancer Res 1989; 49:4682–9.

2. Janes PW, Daly RJ, deFazio A, Sutherland RL. Activation of the Ras signalling pathway in human breast cancer cells overexpressing erbB-2. Oncogene 1994;9:3601–8.

3. Campbell PM, Der CJ. Oncogenic Ras and its role in tumor cell invasion and metastasis. Semin Cancer Biol 2004;14:105–14.

4. Cox AD, Der CJ. The dark side of Ras: regulation of apoptosis. Oncogene 2003;22:8999–9006.

5. Hamad NM, Elconin JH, Karnoub AE, et al. Distinct requirements for Ras oncogenesis in human versus mouse cells. Genes Dev 2002;16: 2045–57.

6. Kolch W. Ras/Raf signalling and emerging pharmacotherapeutic targets. Expert Opin Pharmacother 2002;3:709–18.

7. Kato-Stankiewicz J, Hakimi I, Zhi G, et al. Inhibitors of Ras/Raf-1 interaction identified by two-hybrid screening revert Ras-dependent transformation phenotypes in human cancer cells. Proc Natl Acad Sci U S A 2002;99:14398–403.

8. Lu Y, Sakamuri S, Chen Q-Z, et al. Solution phase parallel synthesis and evaluation of MAPK inhibitory activities of close structural analogues of a Ras pathway modulator. Bioorg Med Chem Lett 2004;14:3957–62.

9. Ihle NT, Paine-Murrieta G, Berggren MI, et al. The phosphatidylinositol-3-kinase inhibitor PX-866 overcomes resistance to the epidermal growth factor receptor inhibitor gefitinib in A-549 human non-small cell lung cancer xenografts. Mol Cancer Ther 2005;4:1349–57.

10. Edwards LA, Verreault M, Thiessen B, et al. Combined inhibition of the phosphatidylinositol 3-kinase/Akt and Ras/mitogen-activated protein kinase pathways results in synergistic effects in glioblastoma cells. Mol Cancer Ther 2006;5:645–54.

11. Ciardiello F, De Vita F, Orditura M, Comunale D, Galizia G. Cetuximab in the treatment of colorectal cancer. Future Oncol 2005;1:173–81.

12. Pegram MD, Lipton A, Hayes DF, et al. Phase II study of receptor-enhanced chemosensitivity using recombinant humanized anti-p185HER2/neu monoclonal antibody plus cisplatin in patients with HER2/neu-overexpressing metastatic breast cancer refractory to chemotherapy treatment. J Clin Oncol 1998;16:2659–71.

13. Plosker GL, Keam SJ. Spotlight on Trastuzumab in the management of HER2-positive metastatic and early-stage breast cancer. BioDrugs 2006;20:259–62.

14. Montaner S, Sodhi A, Molinolo A, et al. Endothelial infection with KSHV genes *in vivo* reveals that vGPCR initiates Kaposi's sarcomagenesis and can promote the tumorigenic potential of viral latent genes. Cancer Cell 2003;3:23–36.

15. Mansour SJ, Matten WT, Hermann AS, et al. Transformation of mammalian cells by constitutively active MAP kinase kinase. Science 1994;265:966–70.

16. Stanton VP, Jr., Nichols DW, Laudano AP, Cooper GM. Definition of the human raf amino-terminal regulatory region by deletion mutagenesis. Mol Cell Biol 1989;9:639–47.

17. Dadke D, Fryer BH, Golemis EA, Field J. Activation of p21-activated kinase 1-nuclear factor κB signaling by Kaposi's sarcoma-associated herpes virus G protein-coupled receptor during cellular transformation. Cancer Res 2003;63:8837–47.

18. Lyons JF, Wilhelm S, Hibner B, Bollag G. Discovery of a novel Raf kinase inhibitor. Endocr Relat Cancer 2001;8:219 – 25.

19. Cox AD, Der CJ. Biological assays for cellular transformation. Methods Enzymol 1994;238:277 – 94.

20. Chou TC, Talalay P. Quantitative analysis of dose-effect relationships: the combined effects of multiple drugs or enzyme inhibitors. Adv Enzyme Regul 1984;22:27 – 55.

21. Gollob JA. Sorafenib: scientific rationales for single-agent and combination therapy in clear-cell renal cell carcinoma. Clin Genitourin Cancer 2005;4:167 – 74.

22. Davies SP, Reddy H, Caivano M, Cohen P. Specificity and mechanism of action of some commonly used protein kinase inhibitors. Biochem J 2000;351:95 – 105.

23. Bhalla US, Ram PT, Iyengar R. MAP kinase phosphatase as a locus of flexibility in a mitogen-activated protein kinase signaling network. Science 2002;297:1018 – 23.

24. Mekhail TM, Markman M. Paclitaxel in cancer therapy. Expert Opin Pharmacother 2002;3:755 – 66.

25. Blagosklonny MV, Schulte T, Nguyen P, Trepel J, Neckers LM. Taxol-induced apoptosis and phosphorylation of Bcl-2 protein involves c-Raf-1 and represents a novel c-Raf-1 signal transduction pathway. Cancer Res 1996;56:1851 – 4.

26. Blagosklonny MV, Giannakakou P, el-Deiry WS, et al. Raf-1/bcl-2 phosphorylation: a step from microtubule damage to cell death. Cancer Res 1997;57:130 – 5.

27. Blagosklonny MV. Sequential activation and inactivation of G2 checkpoints for selective killing of p53-deficient cells by microtubule-active drugs. Oncogene 2002;21:6249 – 54.

28. Britten RA, Perdue S, Opoku J, Craighead P. Paclitaxel is preferentially cytotoxic to human cervical tumor cells with low Raf-1 kinase activity: implications for paclitaxel-based chemoradiation regimens. Radiother Oncol 1998;48:329 – 34.

29. Rasouli-Nia A, Liu D, Perdue S, Britten RA. High Raf-1 kinase activity protects human tumor cells against paclitaxel-induced cytotoxicity. Clin Cancer Res 1998;4:1111 – 6.

30. Britten RA, Perdue S, Eshpeter A, Merriam D. Raf-1 kinase activity predicts for paclitaxel resistance in TP53mut, but not TP53wt human ovarian cancer cells. Oncol Rep 2000;7:821 – 5.

31. Lee M, Koh WS, Han SS. Down-regulation of Raf-1 kinase is associated with paclitaxel resistance in human breast cancer MCF-7/Adr cells. Cancer Lett 2003;193:57 – 64.

32. Abal M, Andreu JM, Barasoain I. Taxanes: microtubule and centrosome targets, and cell cycle dependent mechanisms of action. Curr Cancer Drug Targets 2003;3:193 – 203.

33. Ferlini C, Distefano M, Pignatelli F, et al. Antitumour activity of novel taxanes that act at the same time as cytotoxic agents and P-glycoprotein inhibitors. Br J Cancer 2000;83:1762 – 8.

34. Shields JM, Rogers-Graham K, Der CJ. Loss of transgelin in breast and colon tumors and in RIE-1 cells by Ras deregulation of gene expression through Raf-independent pathways. J Biol Chem 2002;277:9790 – 9.

35. Pruitt K, Pestell RG, Der CJ. Ras inactivation of the retinoblastoma pathway by distinct mechanisms in NIH 3T3 fibroblast and RIE-1 epithelial cells. J Biol Chem 2000;275:40916 – 24.

36. Hamden KE, Whitman AG, Ford PW, Shelton JG, McCubrey JA, Akula SM. Raf and VEGF: emerging therapeutic targets in Kaposi's sarcoma-associated herpesvirus infection and angiogenesis in hematopoietic and nonhematopoietic tumors. Leukemia 2005;19:18 – 26.

37. Hamden KE, Ford PW, Whitman AG, et al. Raf-induced vascular endothelial growth factor augments Kaposi's sarcoma-associated herpesvirus infection. J Virol 2004;78:13381 – 90.

38. Tulpule A, Groopman J, Saville MW, et al. Multicenter trial of low-dose paclitaxel in patients with advanced AIDS-related Kaposi sarcoma. Cancer 2002;95:147 – 54.

39. Bais C, Santomasso B, Coso O, et al. G-protein-coupled receptor of Kaposi's sarcoma-associated herpesvirus is a viral oncogene and angiogenesis activator. Nature 1998;391:86 – 9.

40. Sodhi A, Montaner S, Patel V, et al. Akt plays a central role in sarcomagenesis induced by Kaposi's sarcoma herpesvirus-encoded G protein-coupled receptor. Proc Natl Acad Sci U S A 2004;101:4821 – 6.

41. Jazirehi AR, Vega MI, Chatterjee D, Goodglick L, Bonavida B. Inhibition of the Raf-MEK1/2-ERK1/2 signaling pathway, Bcl-xL down-regulation, and chemosensitization of non-Hodgkin's lymphoma B cells by Rituximab. Cancer Res 2004;64:7117 – 26.

42. Cheung HW, Ling MT, Tsao SW, Wong YC, Wang X. Id-1-induced Raf/MEK pathway activation is essential for its protective role against Taxol-induced apoptosis in nasopharyngeal carcinoma cells. Carcinogenesis 2004;25:881 – 7.

43. O'Neill EE, Matallanas D, Kolch W. Mammalian sterile 20-like kinases in tumor suppression: an emerging pathway. Cancer Res 2005;65:5485 – 7.

44. Carter CA, Chen C, Brink C, et al. Sorafenib is efficacious and tolerated in combination with cytotoxic or cytostatic agents in preclinical models of human non-small cell lung carcinoma. Cancer Chemother Pharmacol 2007;59:183 – 95.

45. Figul M, Soling A, Dong HJ, Chou TC, Rainov NG. Combined effects of temozolomide and the ribonucleotide reductase inhibitors didox and trimidox in malignant brain tumor cells. Cancer Chemother Pharmacol 2003;52:41 – 6.

46. Reynolds CP, Maurer BJ. Evaluating response to antineoplastic drug combinations in tissue culture models. Methods Mol Med 2005;110:173 – 83.